Upper and Lower Bounds for Programmable Vector Fields with Applications to MEMS and Vibratory Plate Parts Feeders

Karl-Friedrich Böhringer, Bruce Randall Donald, Noel C. MacDonald
Cornell University, Ithaca, New York, USA

Programmable vector fields can be used to control a variety of flexible planar parts feeders. These devices can exploit exotic actuation technologies such as arrayed, massively-parallel microfabricated motion pixels or transversely vibrating (macroscopic) plates. These new automation designs promise great flexibility, speed, and dexterity—we believe they may be employed to orient, singulate, sort, feed, and assemble parts. However, since they have only recently been invented, programming and controlling them for manipulation tasks is challenging. When a part is placed on our devices, the programmed vector field induces a force and moment upon it. Over time, the part may come to rest in a dynamic equilibrium state. By chaining together sequences of vector fields, the equilibrium states of a part in the field may be cascaded to obtain a desired final state. The resulting strategies require no sensing and enjoy efficient planning algorithms.

This paper begins by describing our experimental devices. In particular, we describe our progress in building the M-Chip *(Manipulation Chip), a massively parallel array of programmable micro-motion pixels. As proof of concept, we demonstrate a prototype* M-Chip *containing over 11,000 silicon actuators in one square inch. Both the* M-Chip*, as well as macroscopic devices such as transversely vibrating plates, may be programmed with vector fields, and their behavior predicted and controlled using our* equilibrium analysis*. We demonstrate lower bounds (i.e., impossibility results) on what the devices* cannot *do, and results on a* classification of control strategies *yielding design criteria by which well-behaved manipulation strategies may be developed. We provide sufficient conditions for programmable fields to induce well-behaved equilibria on every part. We define* composition operators *to build complex strategies from simple ones, and show the resulting fields are also well-behaved. We discuss whether fields outside this class can be useful and free of pathology.*

Using these tools, we describe new manipulation algorithms. In particular, we improve existing planning algorithms by a quadratic factor, and the plan-length by a linear factor. Using our new and improved strategies, we show how to simultaneously orient and pose any part, without sensing, from an arbitrary initial configuration. We relax earlier dynamic and mechanical assumptions to obtain more robust and flexible strategies.

Finally, we consider parts feeders that can only implement a very limited "vocabulary" of vector fields (as opposed to the pixel-wise programmability assumed above). We show how to plan and execute parts-posing and orienting strategies for these devices, but with a significant increase in planning complexity and some sacrifice in completeness guarantees. We discuss the tradeoff between mechanical complexity and planning complexity.

1 Introduction

Programmable vector fields can be used to control a variety of flexible planar parts feeders. These devices often exploit exotic actuation technologies such as arrayed, microfabricated motion pixels [9, 8, 7] or transversely vibrating plates [4]. These new automation designs promise great flexibility, speed, and dexterity—we believe they may be employed to orient, singulate, sort, feed, and assemble parts (see for example Figures 1 and 4). However, since they have only recently been invented, programming and controlling them for manipulation tasks is challenging. Our research goal is to develop a science base for manipulation using programmable vector fields.

When a part is placed on our devices, the programmed vector field induces a force and moment upon it. Over time, the part may come to rest in a dynamic equilibrium state. In principle, we have tremendous flexibility in choosing the vector field, since using

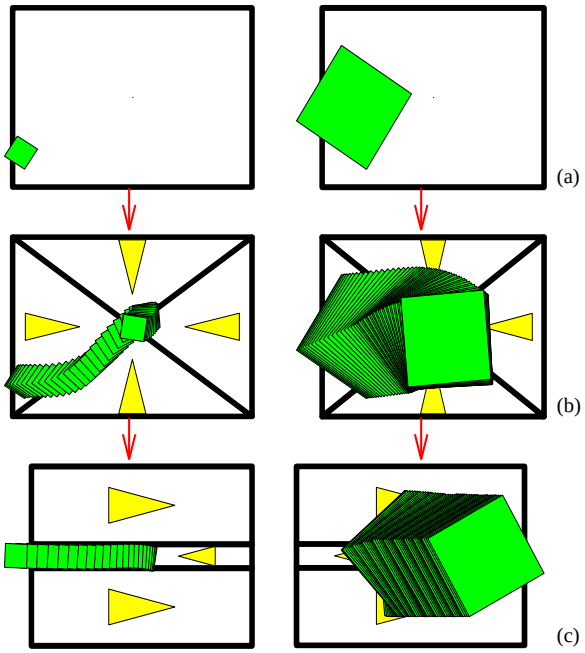

Figure 1: *Sensorless sorting using force vector fields: parts of different sizes are first centered and subsequently separated depending on their size.*

modern array technologies, the force field may be programmed pixel-wise. Hence, we have a lot of control over the resulting equilibrium states. By chaining together sequences of vector fields, the equilibria may be cascaded to obtain a desired final state—for example, this state may represent a unique orientation or pose of the part. A system with such a behavior exhibits the *feeding property* [2]:

> A system has the *feeding property* over a set of parts $\mathcal{P}$ and a set of initial configurations $\mathcal{I}$ if, given any part $P \in \mathcal{P}$, there is some output configuration $\mathbf{q}$ such that the system can move P to $\mathbf{q}$ from any location in $\mathcal{I}$.

Our work on programmable vector fields is related to nonprehensile manipulation [17, 44, 22, 20]: in either case, parts are manipulated without form or force closure.

This paper first describes our experimental devices, a technique for analyzing them called *equilibrium analysis*, lower bounds (i.e., impossibility results) on what the devices *cannot* do, and results on a classification of control strategies yielding design criteria by which well-behaved manipulation strategies may be developed. Then we describe new manipulation algorithms using these tools. In particular, we improve existing planning algorithms by a quadratic factor, show how to simultaneously orient and pose a part, and we relax earlier dynamic and mechanical assumptions to obtain more robust and flexible strategies.

We pose the question *Which vector fields are suitable for manipulation strategies?* In particular, we ask whether the fields may be *classified*. That is: can we characterize all those vector fields in which every part has stable equilibria? While this question has been well-studied for a point mass in a field, the issue is more subtle when lifted to a body with finite area, due to the moment covector. To answer, we first demonstrate impossibility results, in the form of "lower bounds:" there exist perfectly plausible fields which induce *no* stable equilibrium in very simple parts.

Fortunately, there is also good news. We present conditions for fields to induce well-behaved equilibria when lifted, by exploiting the theory of potential fields. While potential fields have been widely used in robot control [30, 39, 38], micro-actuator arrays present us with the ability to *explicitly* program the applied force *at every point* in a vector field. Whereas previous work has developed control strategies with *artificial* potential fields, our fields are non-artificial (i.e., physical). This alone makes our application of potential field theory to micro-devices unique and novel. Moreover, such fields can be composed using addition, sequential composition, "parallel" composition by superposition of controls, or by a new kind of "morphing" of control signals which we will define.

Finally, the desire to implement complicated fields raises the question of control uncertainty. We close by describing how families of potential functions can be used to represent control uncertainty, and analyzed for their impact on equilibria, and we will give an outlook on still open problems and future work.

Because of limited space, we have abbreviated or omitted some of the proofs of our propositions. For a more detailed discussion please refer to the on-line version of our long paper at URL `http://www.cs.cornell.edu/home/karl/ProgVecFields`, or to [3].

2 Experimental Apparatus: Parts Feeders

It is often extremely costly to maintain part order throughout the manufacture cycle. For example, instead of keeping parts in pallets, they are often delivered in bags or boxes, whence they must be picked out and sorted. A parts feeder is a machine that orients such parts before they are fed to an assembly station. Currently, the design of parts feeders is a black art that is responsible for up to 30% of the cost and 50% of workcell failures [10, for example]. Thus although part feeding accounts for a large portion of assembly cost, there is not much scientific basis for automating the process.

The most common type of parts feeder is the *vibratory bowl feeder*, where parts in a bowl are vibrated using a rotary motion, so that they climb a helical track. As they climb, a sequence of baffles and cutouts in the track create a mechanical "filter" that causes parts in all but one orientation to fall back into the bowl for another attempt at running the gauntlet [10]. Sony's APOS parts feeder [27] uses an array of nests (silhouette traps) cut into a vibrating plate. The nests and the vibratory motion are designed so that the part will remain in the nest only in a particular orientation. By tilting the plate and letting parts flow across it, the nests eventually fill up with parts in the desired orientation. Although the vibratory motion is under software control, specialized mechanical nests must be designed for each part [36].

The reason for the success of vibratory bowl feeders and the Sony APOS system is the underlying principle of *sensorless manipulation* [21] that allows parts positioning and orienting without sensor feedback. This principle is even more important at small scales, because sensor data will be less accurate and more difficult to obtain. The APOS system or bowl feeders are unlikely to work in the micro domain: instead novel device designs for micro-manipulation tasks are required. The theory of sensorless manipulation is the science base for developing and controlling such devices.

Reducing the amount of required sensing is an example of *minimalism* [5, 14], which pursues the following agenda: For a given robot task, find the minimal configuration of resources required to solve the task. Minimalism is interesting because doing task A without resource B proves that B is somehow inessential to the information structure of the task. In robotics, minimalism has become increasingly influential. Raibert [37] showed that walking and running machines could be built without static stability. Erdmann and Mason [21] showed how to do dexterous manipulation without sensing. McGeer [34] built a biped, kneed walker without sensors, computers, or actuators. Canny and Goldberg [14] argue that minimalism has a long tradition in industrial manufacturing, and developed geometric algorithms for orienting parts using simple grippers and accurate, low cost light beams. Brooks [12] has developed online algorithms that rely less extensively on planning and world models. Donald et al. [17, 5] have built distributed teams of mobile robots that cooperate in manipulation without explicit communication. We intend to use these results for our experiments in micro-manipulation, and to examine how they relate to our theoretical proofs of minimalist systems.

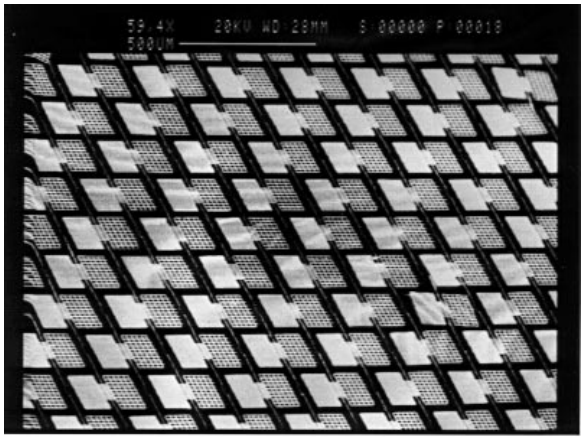

Figure 2: *A prototype* M-Chip *fabricated in 1995. A large unidirectional actuator array (scanning electron microscopy). Each actuator is* $180 \times 240\,\mu m^2$ *in size. Detail from a* $1\,in^2$ *array with more than 11,000 actuators. For more pictures on device design and fabrication see URL* `http://www.cs.cornell.edu/home/karl/MicroActuators`.

2.1 Microfabricated Actuator Arrays

A wide variety of micromechanical structures (devices with features in the μm range) has been built recently by using processing techniques known from VLSI in-

dustry. However, the fabrication, control, and programming of micro-devices that can interact and actively change their environment remains challenging. Problems arise from

1. unknown material properties and the lack of adequate models for mechanisms at very small scales,
2. the limited range of motion and force that can be generated with microactuators,
3. the lack of sufficient sensor information with regard to manipulation tasks, and
4. design limitations and geometric tolerances due to the fabrication process.

MEMS manipulator arrays have been proposed by several MEMS researchers, among others Fujita et al. [24], Will et al. [31], or Suh et al. [42]. For an overview see [31] or [9, 8]. Our arrays (Figure 2) are fabricated using a SCREAM (Single-Crystal Reactive Etching and Metallization) process developed in the Cornell Nanofabrication Facility [43, 41]. The SCREAM process is low-temperature, and does not interfere with traditional VLSI [40]. Hence it opens the door to building monolithic microelectromechanical systems with integrated microactuators and control circuitry on the same wafer.

Our design is based on microfabricated torsional resonators [35]. Each unit device consists of a rectangular grid etched out of single-crystal silicon suspended by two rods that act as torsional springs (Figure 2). The grid is about 200 μm long and extends 120 μm on each side of the rod. The rods are 150 μm long. The current asymmetric design has 5 μm high protruding tips on one side of the grid that make contact with an object lying on top of the actuator. The other side of the actuator consists of a denser grid above an aluminum electrode. If a voltage is applied between silicon substrate and electrode, the dense grid above the electrode is pulled downward by the resulting electrostatic force. Simultaneously the other side of the device (with the tips) is deflected out of the plane by several μm. Hence an object can be lifted and pushed sideways by the actuator.

The fabrication process and mechanism analysis are described in more detail in [9, 8, 7].

2.2 Macroscopic Vibratory Parts Feeder

Böhringer et al. [4] have presented a device that uses the force field created by transverse vibrations of a plate to position and align parts. The device consists of an aluminum plate that is attached to a commercially available electrodynamic vibration generator,[1] with a linear travel of 0.02 m, and capable of producing a force of up to 500 N (Figure 3). The input signal, specifying the waveform corresponding to the desired oscillations, is fed to a single coil armature, which moves in a constant field produced by a ceramic permanent magnet in a center gap configuration.

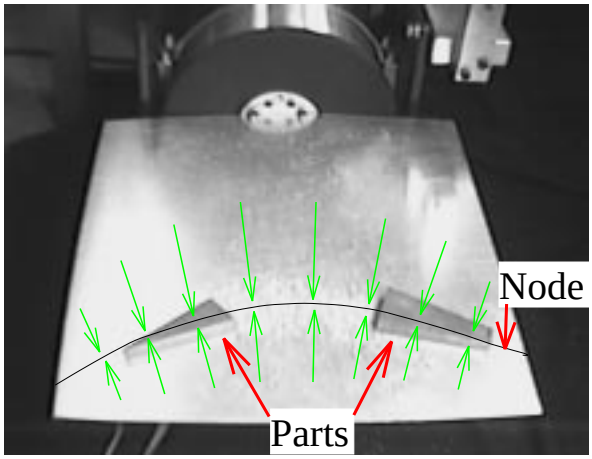

Figure 3: *Vibratory parts feeder: an aluminum plate (size 50 cm × 40 cm) exhibits a vibratory minimum. Parts are attracted to this* nodal line *and reach equilibrium there. See also URL* `http://www.cs.cornell.edu/home/karl/VibratoryAlign`. *Reproduced with permission from [4].*

For low amplitudes and frequencies, the plate moves longitudinally with no perceptible transverse vibrations. However, as the frequency of oscillations is increased, transverse vibrations of the plate become more pronounced. The resulting motion is similar to the forced transverse vibration of a rectangular plate, clamped on one edge and free along the other three sides. This vibratory motion creates a force field in which particles are attracted to locations with minimal vibration, called the *nodal lines*. This field can be programmed by changing the frequency, or by employing clamps as programmable fixtures that create various vibratory nodes.

[1] Model VT-100G, Vibration Test Systems, Akron, OH, USA.

Figure 3 shows two parts, shaped like a triangle and a trapezoid, after they have reached their stable poses. To better illustrate the orienting effect, the curve showing the nodal line has been drawn by hand. *Nota bene*: This device can only use the finite manipulation grammar described in Section 6.2 since it can only generate a constrained set of vibratory patterns, and cannot implement radial strategies.

3 Equilibrium Analysis For Programmable Vector Fields

For the generation of manipulation strategies with programmable vector fields it is essential to be able to predict the motion of a part in the field. Particularly important is determining the stable equilibrium poses a part can reach in which all forces and moments are balanced. This *equilibrium analysis* was introduced in our short conference paper [8], where we presented a theory of manipulation for programmable vector fields, and an algorithm that generates manipulation strategies to orient polygonal parts without sensor feedback using a sequence of *squeeze fields*.

We now review the algorithm in [8] and give a detailed proof of its complexity bounds. The tools developed here are essential to understanding our new and improved results.

3.1 Squeeze Fields and Equilibria

In [8] we proposed a family of control strategies called *squeeze fields* and a planning algorithm for parts-orientation.

Definition 1 [8] *Assume l is a straight line through the origin. A* squeeze field *F is a two-dimensional force field defined as follows:*

1. *If $z \in \mathbb{R}^2$ lies on l then $f(z) = 0$.*
2. *If z does not lie on l then $f(z)$ is the unit vector normal to l and pointing towards l.*

We refer to the line l as the *squeeze line*, because l lies in the center of the squeeze field. See Figure 4 for examples of squeeze fields.

Assuming quasi-static motion, a small object will move perpendicularly towards the line l and come to rest there. We are interested in the motion of an arbitrarily shaped (not necessarily small) part P. Let us

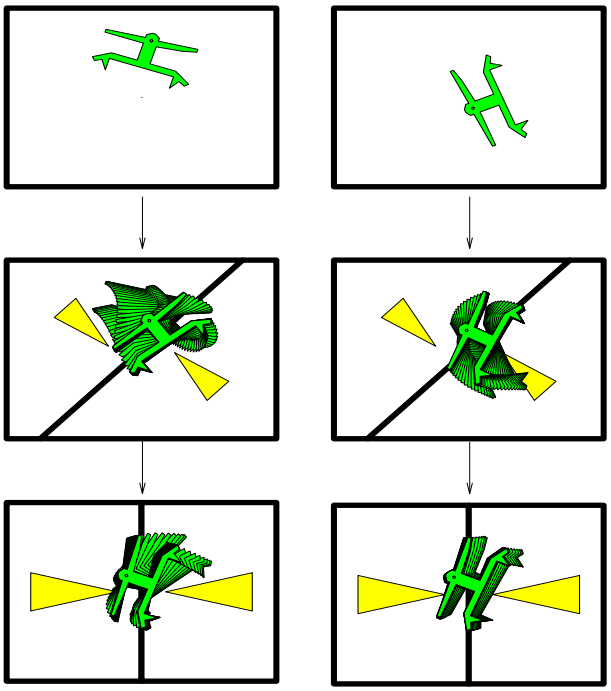

Figure 4: *Sensorless parts alignment using force vector fields: The part reaches unique orientation after two subsequent squeezes. There exist such alignment strategies for all polygonal parts. See URL* `http://www.cs.cornell.edu/home/karl/MicroManipulation` *for an animated simulation.*

call P_1, P_2 the regions of P that lie to the left and to the right of l, respectively, and C_1, C_2 their centers of mass. In a rest position both translational and rotational forces must be in equilibrium. We obtain the following two conditions:

I: The areas P_1 and P_2 must be equal.
II: The vector $C_2 - C_1$ must be normal to l.

P has a translational motion component normal to l if **I** does not hold. P has a rotational motion component if **II** does not hold. This assumes a uniform force distribution over the surface of P, which is a reasonable assumption for a flat part that is in contact with a large number of elastic actuators.

Definition 2 *A part P is in* translational equilibrium *if the forces acting on P are balanced. P is in* orientational equilibrium *if the moments acting on P are balanced.* Total equilibrium *is simultaneous translational*

and orientational equilibrium.

Let (x_0, y_0, θ_0) be an equilibrium pose of P. (x_0, y_0) is the corresponding translation equilibrium*, and θ_0 is the corresponding* orientation equilibrium*.*

Note that conditions **I** and **II** do *not* imply that in equilibrium, the center of area of P has to coincide with the squeeze line l. For example, consider a large and a small square connected by a long rod of negligible width. If the rod is long enough, the center of area will lie outside of the large square. However, in equilibrium the squeeze line l will always intersect the large square.

Definition 3 *A* bisector *of a polygon P is a line that cuts P into two sections of equal size.*

Proposition 4 *Let P be a polygon whose interior is connected. There exist $O(kn^2)$ bisectors such that P is in equilibrium when placed in a squeeze field such that the bisector coincides with the squeeze line. n is the part complexity measured as the number of polygon vertices. k denotes the maximum number of polygon edges that a bisector can cross.*

If P is convex, then the number of bisectors is bounded by $O(n)$.

Proof: See URL `http://www.cs.cornell.edu/home/karl/ProgVecFields`, or [3]. □

For most part geometries, k is a small constant.[2] However in the worst-case, pathological parts can reach $k = O(n)$. A (e.g. rectilinear) spiral-shaped part would be an example for such a pathological case, because every bisector intersects $O(n)$ polygon edges.

3.2 Planning of Manipulation Strategies

In this section we present an algorithm for sensorless parts alignment with squeeze fields [8]. Recall from Section 3.1 that in squeeze fields, the equilibria for connected polygons are discrete (except for a neutrally stable translation parallel to the squeeze line which we will disregard for the remainder of Section 3).

To model our actuator arrays and vibratory devices, in [8] we made the following assumptions:

DENSITY: The generated forces can be described by a vector field, i.e. the individual microactuators are dense compared to the size of the moving part.

[2] In particular, in [8] we assumed that $k = O(1)$.

2PHASE: The motion of a part has two phases: (1) Pure translation towards l until the part is in translational equilibrium. (2) Motion in translational equilibrium until orientational equilibrium is reached.

Note that due to the elasticity and oscillation of the actuator surfaces, we can assume continuous area contact, and not just contact in three or a few points. If a part moves while in translational equilibrium, in general the motion is not a pure rotation, but also has a translational component. Therefore, relaxing assumption 2PHASE is one of the key results of this paper.

Definition 5 **[8]** *Let θ be the orientation of a connected polygon P in a squeeze field, and let us assume that condition* **I** *holds. The* turn function $t : \theta \to \{-1, 0, 1\}$ *describes the instantaneous rotational motion of P:*

$$t(\theta) = \begin{cases} 1 & \text{if } P \text{ will turn counterclockwise} \\ -1 & \text{if } P \text{ will turn clockwise} \\ 0 & \text{if } P \text{ is in total equilibrium (Fig. 5).} \end{cases}$$

This definition immediately implies the following lemma:

Lemma 6 **[8]** *Let P be a polygon with orientation θ in a squeeze field such that condition* **I** *holds. P is stable if $t(\theta) = 0$, $t(\theta+) \leq 0$, and $t(\theta-) \geq 0$. Otherwise P is unstable.*

Proof: Assume the part P is in a pose (x, y, θ) such that condition **I** is satisfied. This implies that the translational forces acting on P balance out. If in addition $t(\theta) = 0$, then the effective moment is zero, and P is in total equilibrium. Now consider a small perturbation $\delta\theta > 0$ of the orientation θ of P while condition **I** is still satisfied. For a stable equilibrium, the moment resulting from the perturbation $\delta\theta$ must not aggravate but rather counteract the perturbation. This is true if and only if $t(\theta + \delta\theta) \leq 0$ and $t(\theta - \delta\theta) \geq 0$. □

Using this lemma we can identify all stable orientations, which allows us to construct the squeeze function [25] of P (see Figure 5c), i.e. the mapping from an initial orientation of P to the stable equilibrium orientation that it will reach in the squeeze field:

Lemma 7 **[8]** *Let P be a polygonal part on an actuator array A such that assumptions* DENSITY *and* 2PHASE *hold. Given the turn function t of P, its corresponding* squeeze function $s : \mathbb{S}^1 \to \mathbb{S}^1$ *is constructed as follows:*

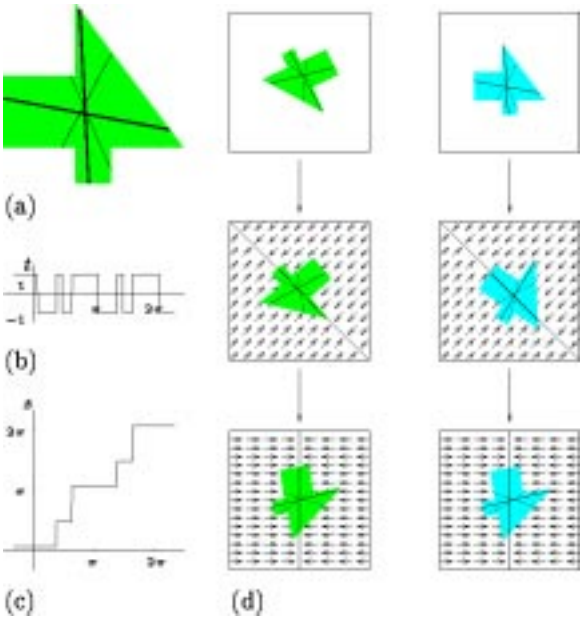

Figure 5: *(a) Polygonal part. Stable (thick line) and unstable (thin line) bisectors are also shown. (b) Turn function, which predicts the orientations of the stable and unstable bisectors. (c) Squeeze function, constructed from the turn function. (d) Alignment strategy for two arbitrary initial configurations. See URL* `http://www.cs.cornell.edu/home/karl/Cinema` *for an animated simulation.*

1. *All stable equilibrium orientations θ map identically to θ.*
2. *All unstable equilibrium orientations map (by convention) to the nearest counterclockwise stable orientation.*
3. *All orientations θ with $t(\theta) = 1$ (-1) map to the nearest counterclockwise (clockwise) stable orientation.*

Then s describes the orientation transition of P induced by A.

Proof: Assume that part P initially is in pose (x, y, θ) in array A. Because of 2PHASE, we can assume that P translates towards the center line l until condition **I** is satisfied without changing its orientation θ. P will change its orientation until the moment is zero, i.e. $t = 0$: A positive moment ($t > 0$) causes counterclockwise motion, and a negative moment ($t < 0$) causes clockwise motion until the next root of t is reached. □

We conclude that any connected polygonal part, when put in a squeeze field, reaches one of a *finite* number of possible orientation equilibria [8]. The motion of the part and, in particular, the mapping between initial orientation and equilibrium orientation is described by the squeeze function, which is derived from the turn function as described in Lemma 7. Note that all squeeze functions derived from turn functions are monotone step-shaped functions.

Goldberg [25] has given an algorithm that automatically synthesizes a manipulation strategy to uniquely orient a part, given its squeeze function. While Goldberg's algorithm was designed for squeezes with a robotic parallel-jaw gripper, in fact, it is more general, and can be used for arbitrary monotone step-shaped squeeze functions. The output of Goldberg's algorithm is a sequence of angles that specify the required directions of the squeezes. Hence these angles specify the direction of the squeeze line in our force vector fields (for example the two-step strategy in Figures 4 and 5d).

It is important to note that the equilibria obtained by a MEMS squeeze field and by a parallel-jaw gripper will typically be different, even when the squeeze directions are identical. For example, to see this, consider squeezing a square-shaped part. Stable and unstable equilibria are switched. This shows that our mechanical analysis of equilibrium is different from that of the parallel-jaw gripper. Let us summarize these results:

Theorem 8 **[8]** *Let P be a polygon whose interior is connected. There exists an alignment strategy consisting of a sequence of squeeze fields that uniquely orients P up to symmetries.*

Corollary 9 *The alignment strategies of Theorem 8 have $O(k\,n^2)$ steps, and they may be computed in time $O(k^2\,n^4)$, where k is the maximum number of edges that a bisector of P can cross. In the case where P is convex, the alignment strategy has $O(n)$ steps and can be computed in time $O(n^2)$.*

Proof: Proposition 4 states that a polygon with n vertices has $E = O(k\,n^2)$ stable orientation equilibria in a squeeze field ($O(n)$ if P is convex). This means that the image of its corresponding squeeze function is a set of E discrete values. Given such a squeeze function, Goldberg's algorithm [25] constructs alignment strategies with $O(E)$ steps. Planning complexity is $O(E^2)$. □

Goldberg's strategies [25] have the same complexity bounds for convex and non-convex parts, because when using squeeze grasps with a parallel-jaw gripper, only the convex hull of the part need be considered. This is not the case for programmable vector fields, where manipulation strategies for non-convex parts are more expensive. As described in Section 3.1, there could be parts that have $E = \Omega(k\,n^2)$ orientation equilibria in a squeeze field, which would imply alignment strategies of length $\Omega(k\,n^2)$ and planning complexity $\Omega(k^2\,n^4)$. In Section 6.1 we will present new and improved manipulation algorithms that reduce the number of equilibria to $E = O(k\,n)$.

This scheme may be generalized to the case where l is slightly curved, as in the "node" of the vibrating plate in Figure 3. See [4] for details. The remaining sections of this paper investigate using more exotic fields (not simple squeeze patterns) to

1. allow disconnected polygons,
2. relax assumption 2PHASE,
3. reduce the planning complexity,
4. reduce the number of equilibria,
5. reduce the execution complexity (strategy length), and
6. determine feasibility results and limitations for manipulation with general force fields.

3.3 Relaxing the 2PHASE Assumption

In Section 3.2, assumption 2PHASE allowed us to determine successive equilibrium positions in a sequence of squeezes, by a quasi-static analysis that decouples translational and rotational motion of the moving part. For any part, this provides a *unique* orientation equilibrium (after several steps). If 2PHASE is relaxed, we obtain a dynamic manipulation problem, in which we must determine the equilibria (x, θ) given by the part orientation θ and the offset x of its center of mass from the squeeze line. A stable equilibrium is a (x_i, θ_i) pair in $\mathbb{R} \times \mathbb{S}^1$ that acts as an *attractor* (the x offset in an equilibrium is, surprisingly, usually not 0). Again, we can compute these (x_i, θ_i) equilibrium pairs *exactly*, as outlined in Section 3.1.

Considering (x_i, θ_i) equilibrium pairs has another advantage. We can show that, even without 2PHASE, after two successive, orthogonal squeezes, the set of stable poses of any part can be reduced from $\mathcal{C} = \mathbb{R}^2 \times \mathbb{S}^1$ to a *finite* subset of $\mathcal{C}$ (the configuration space of part P); see Claim 28 below. Subsequent squeezes will preserve the finiteness of the state space. This will significantly reduce the complexity of a task-level motion planner. Hence if assumption 2PHASE is relaxed, this idea still enables us to simplify the general motion planning problem (as formulated e.g. by Lozano-Pérez, Mason, and Taylor in [33]) to that of Erdmann and Mason [21]. Conversely, relaxing assumption 2PHASE raises the complexity from the "linear" planning scheme of Goldberg [25] to the forward-chaining searches of Erdmann and Mason [21], or Donald [16].

4 Lower Bounds: What Programmable Vector Fields Cannot Do

We now present "lower bounds" — constituting vector fields and parts with pathological behavior, making them unusable for manipulation. These counterexamples show that we must be careful in choosing programmable vector fields, and that, *a priori*, it is not obvious when a field is well-behaved.

In Section 3 we saw that in a vector field with a simple squeeze pattern (see again Figure 4), polygonal parts reach certain equilibrium poses. This raises the question of a *general classification of all those vector fields in which every part has stable equilibria.* There exist vector fields that do not have this property even though they are very similar to a simple squeeze.

Definition 10 *A* skewed field f_S *is a force vector field given by* $f_S(x, y) = -\text{sign}(x)(1, \epsilon)$, *where* $0 \neq \epsilon \in \mathbb{R}$.

Proposition 11 *A skewed vector field induces* no *stable equilibrium on a disk-shaped part.*

Proof: Consider Figure 6, which shows a skewed field with $\epsilon = -\frac{2}{3}$: Only when the center of the disk coincides with the center of the squeeze pattern do the translational forces acting on the disk balance. But it will still experience a positive moment that will cause rotation. □

Similarly we would like to identify the *class of all those parts that always reach stable equilibria* in particular vector fields. From Section 3 we know that connected polygons in simple squeeze fields satisfy this condition. This property relies on finite area contacts: it does not hold for point contacts. As a counterexample consider the part in Figure 7.

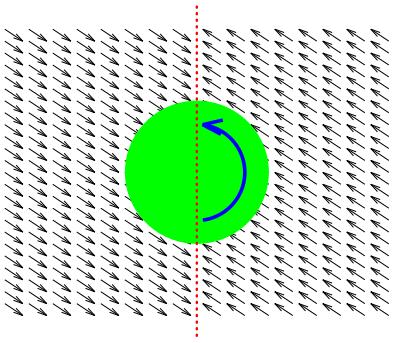

Figure 6: *Unstable part in the skewed squeeze field ($\epsilon = -\frac{2}{3}$). The disk with center on the squeeze line will keep rotating. Moreover, it has* no *stable equilibrium in this field.*

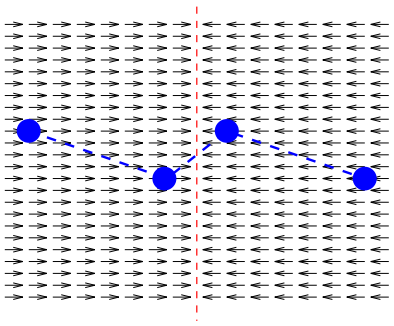

Figure 7: *S-shaped part with four rigidly connected point-contact "feet" in unstable total equilibrium (forces and moments balance). There exists* no *stable equilibrium position for this part in a vector field with a simple squeeze pattern. For an animation see URL* `http://www.cs.cornell.edu/home/karl/MicroManipulation/Patho`.

Proposition 12 *There exist parts that do not have stable equilibria in a simple squeeze field.*

Proof: The S-shaped part in Figure 7 has four rigidly connected "feet" with small contact surfaces. As the area of each of these four feet approaches zero, the part has *no* stable equilibrium in a simple squeeze field. There is only one orientation for the part in which both force and moment balances out, and this orientation is unstable. □

Finally, the *number of stable equilibria* of a given part influences both the planning complexity and the plan length of an alignment strategy. It also affects the resolution of the vector field that is necessary to perform a strategy accurately. Even though all parts we have considered exhibit only one or two orientation equilibria, there exist no tight bounds on the maximum number of orientation equilibria in a unit squeeze field.

Proposition 13 *Let n be the number of vertices of a polygon P, and let k be the maximum number of edges that a bisector of P can cross:*

A. Regular polygons have n stable orientation equilibria in a squeeze field.
B. Every connected polygon has $O(k\,n^2)$ stable orientation equilibria in a squeeze field.

Proof:

A. Because of their part symmetry, regular polygons have $2n$ equilibria. Half of them are stable, the other n are unstable.
B. See Section 3.1.

□

As described in Section 3.1, there exist simple polygons with n vertices that can be bisected by a straight line in up to $O(k\,n^2)$ topologically different ways [6]. This suggests that there could be parts that have $\Omega(k\,n^2)$ orientation equilibria in a squeeze field, which would imply alignment strategies of length $\Omega(k\,n^2)$ and planning complexity $\Omega(k^2\,n^4)$.

While the counterexample in Figure 7 may be plausibly avoided by prohibiting parts with "point contacts," the other examples (Figure 6 and Proposition 13B) are more problematic. In Section 5, we show how to choose programmable vector fields that exclude some of these pathological behaviors, by using the *theory of potential fields* to describe a class of force vector fields for which *all* polygonal parts have stable equilibria. In Section 6.1, we show how to combine these fields to obtain new fields in which all parts have only $O(k\,n)$ equilibria.

We believe parts with point contact (not having finite area contact) will behave badly in *all* vector fields. We can model a point contact with delta functions, such that e.g. for a point contact P_0 at (x_0, y_0): $\int_{P_0} f\ dA = \int f\ \delta(x_0, y_0)\ dA = f(x_0, y_0)$. This model is frequently used in mechanics (see e.g. [19]). Point contact permits rapid, discontinuous changes in force and moment. Hence, bodies with point contact will tend to exhibit instabilities, as opposed to flat parts

that are in contact with a large number of (elastic) actuators. Finally, we believe that as the area contact—the size of the "feet" of a part—approaches zero, the part may become unstable. This represents a design constraint on parts which are to be manipulated using programmable planar parts feeders.

The lower bounds we demonstrate are indications of the pathologies that can arise when fields without potential or parts with point contact are permitted. Each of our counterexamples (Figures 6 and 7) is "generic" in that it can be generalized to a very large class of similar examples. However, these lower bounds are just a first step, and one wishes for examples that delineate the capabilities of programmable vector fields for planar parts manipulation even more precisely.

The separating field shown in Figure 1c is not a potential field, and that there exist parts that will spin forever, without equilibrium, in this field (this follows by generalizing the construction in Figure 6). However, for *specific parts*, such as those shown in Figure 1, this field is useful if we can pose the parts appropriately first (e.g., using the potential field shown in Figure 1b).

Finally, we may "surround" non-potential fields with potential fields to obtain reasonable behavior in some cases. Figure 1 shows how to "surround" a non-potential field in *time* by potential fields, to eliminate pathologies. Similarly, we can surround non-potential fields *spatially*. For example, if field 1c could be surrounded by a larger potential field, then after separation, parts can reach a stable equilibrium.

Non-potential fields can be used safely with the following methodology: Let $H \subset \mathcal{C} = \mathbb{R}^2 \times \mathbb{S}^1$ be the undesirable limit set. For example, H could be a limit cycle where the part spins forever. Let $\widehat{P}_V(H)$ be the weak pre-image [33, 15] of H under the field V. If we can ensure that the part starts in a configuration $z \notin \widehat{P}_V(H)$, it will not reach the unwanted limit cycle. For example, in Figure 1 the centering step (b) ensures that the part does not end up on the border between the two separating fields, where it would spin forever in step (c).

5 Completeness: Classification Using Potential Fields

We are interested in a *general classification of all those vector fields in which every part has stable equilibria.* As motivation, recall that a skewed vector field, even though very similar to a regular squeeze field (see again Figure 4), induces *no* stable equilibrium in a disk-shaped part (Figure 6). In this section we give a family of vector fields that will be useful for manipulation tasks. These fields belong to a specific class of vector fields: the class of fields that have a potential.

We believe that fields without potential will often induce pathological behavior in many parts. Fields without potential admit paths along which a particle (point mass) will gain energy. Since mechanical parts are rigid aggregations of particles, this may induce unstable behavior in larger bodies. However, there are some cases where non-potential fields may be useful. For example, see Figure 1c, which is *not* a potential field. Such fields may be employed to *separate* but not to stabilize, pose, or orient parts. This strong statement devolves to our proof that fields like Figure 6 do not have well-behaved equilibria. Hence, they should only be employed when we want to induce an unstable system that will cast parts away from equilibrium, e.g. in order to sort or separate them.

Consider the class of vector fields on $\mathbb{R}^2$ that have a *potential*, i.e. fields f in which the work is independent of the path, or equivalently, the work on any closed path is zero, $\oint f \cdot ds = 0$. In a potential field each point (x, y) is assigned a real value $U(x, y)$ that can be interpreted as its potential energy. When U is smooth, then the vector field f associated with U is the gradient $-\nabla U$. In general, $U(x, y)$ is given, up to an additive constant, by the path integral $\int_\alpha f \cdot ds$ (when it exists and it is unique), where α is an arbitrary path from a fixed reference point (x_0, y_0) to (x, y).

An ideal point object is in stable equilibrium if and only if it is at a local minimum of U.

Definition 14 *Let f be a force vector field on $\mathbb{R}^2$, and let $\mathbf{p}$ be a point that is offset from a fixed reference point $\mathbf{q}$ by a vector $\mathbf{r}(\mathbf{p}) = \mathbf{p} - \mathbf{q}$. We define the* generalized force *F as the force* and *moment induced by f at point $\mathbf{p}$:*

$$F(\mathbf{p}) \quad = \quad (f(\mathbf{p}) \ , \ \mathbf{r}(\mathbf{p}) \times f(\mathbf{p})) \qquad (1)$$

Let P be a part of arbitrary shape, and let $P_\mathbf{z}$ denote the part P in pose $\mathbf{z} = (x, y, \theta) \in \mathcal{C}$. We define the lifted

force field f_P *as the area integral of the force induced by* f *over* $P_{\mathbf{z}}$*:*

$$f_P(\mathbf{z}) \quad = \quad \int_{P_{\mathbf{z}}} f \; dA \tag{2}$$

The lifted generalized force field F_P *is defined as the area integral of the force* and *moment induced by* f *over* P *in configuration* $\mathbf{z}$*:*

$$\begin{aligned} F_P(\mathbf{z}) \quad &= \quad \int_{P_{\mathbf{z}}} F \; dA \\ &= \quad \left(\int_{P_{\mathbf{z}}} f \; dA \; , \; \int_{P_{\mathbf{z}}} \mathbf{r} \times f \; dA \right) \end{aligned} \tag{3}$$

Hence, F_P *is a vector field on* $\mathcal{C}$*. Finally, we define the* lifted potential $U_P : \mathcal{C} \to \mathbb{R}$*.* U_P *is the area integral of the potential* U *over* P *in configuration* $\mathbf{z}$*:*

$$U_P(\mathbf{z}) \quad = \quad \int_{P_{\mathbf{z}}} U \; dA \tag{4}$$

We now show that the category of potential fields is closed under the operation of lifting, and that U_P is the potential of F_P . Note that U need not be smooth.

Let $g : X \to Y$ and $h : Y \to Z$. Let $k : X \to Z$ be the function which is the composition of g and h, defined by $k(x) = h(g(x))$. In the following proposition, we use the notation $h(g)$ to denote k, the function composition of g and h.

Proposition 15 *Let* f *be a force field on* $\mathbb{R}^2$ *with potential* U*, and let* P *be a part of arbitrary shape. For the lifted generalized force field* F_P *and the lifted potential* U_P *the following equality holds:* $U_P = \int_P U \; dA = \int_\alpha F_P \cdot d\mathbf{z} + c$*, where* α *is an arbitrary path in* $\mathcal{C}$ *from a fixed reference point, and* c *is a constant.*

Proof: See URL `http://www.cs.cornell.edu/home/karl/ProgVecFields`, or [3]. □

So again, $U_P(x, y, \theta)$ can be interpreted as the potential energy of part P in configuration (x, y, θ). Therefore we obtain a lifted potential field U_P whose local minima are the stable equilibrium configurations in $\mathcal{C}$ for part P. Furthermore, potential fields are closed under addition and scaling. We can thus create and analyze more complex fields by looking at their components. In general, the theory of potential fields allows us to classify manipulation strategies with vector fields, offering new insights into equilibrium analysis and providing the means to determine strategies with stable equilibria. For example, it allows us to show that orientation equilibrium in a simple squeeze field is equivalent to the stability of a homogeneous boat floating in water, provided its density is $\rho = \frac{1}{2}\rho_{\text{water}}$.

5.1 Examples: Classification of Force Fields

Example: Radial fields. A *radial field* is a vector field whose forces are directed towards a specific center point. It can be used to center a part in the plane. The field in Figure 1b can be understood as a radial field with a rather coarse discretization using only four different force directions. Note that this field has a potential.

As a specific example for radial fields, consider the *unit radial field* R which is defined by $R(\mathbf{z}) = -\mathbf{z}/||\mathbf{z}||$ for $\mathbf{z} \neq \mathbf{0}$, and $R(\mathbf{0}) = \mathbf{0}$. Note that R has a discontinuity at the origin. A smooth radial field can be defined, for example, by $R'(\mathbf{z}) = -\mathbf{z}$. The corresponding potential fields are $U(\mathbf{z}) = ||\mathbf{z}||$, and $U'(\mathbf{z}) = \frac{1}{2}||\mathbf{z}||^2$, respectively. Note that U is continuous (but not smooth), while U' is smooth.

Counterexample: Skewed squeeze fields. Consider again the *skewed squeeze field* in Figure 6. This is not a potential field, which explains why the disk-shaped part has no equilibrium: Note that for example the integral on a cyclic path along the boundary of the disk is non-zero.

Example: Morphing and combining vector fields. Our strategies from [8] (see Section 3) have *switch points* in time where the vector field changes discontinuously (Figure 4). This is because after one squeeze, for every part, the orientation equilibria form a finite set of possible configurations, but in general there exists no unique equilibrium (as shown in Section 3.2). Hence subsequent squeezes are needed to disambiguate the part orientation. Therefore these switches are necessary for strategies with squeeze patterns.

One may ask whether, using another class of potential field strategies, *unique* equilibria may be obtained without discrete switching. We believe that *continuously varying* vector fields of the form $(1 - t)f + t\,g$, where $t \in [0, 1]$ represents time, and f and g are

squeezes, may lead to vector fields that have this property. Here "+" denotes point-wise addition of vector fields, and we will write "$f \rightsquigarrow g$" for the resulting continuously varying field. By restricting f and g to be fields with potentials U and V, we know that $U + V$ and $(1-t)U + tV$ are potential fields, and hence we can guarantee that $f + g$ and $f \rightsquigarrow g$ are well-behaved strategies. These form the basis of our new algorithms in Section 6.

Let us formalize the previous paragraphs. If f is a vector field (in this case a squeeze pattern) that is applied to move part P, we define the *equilibrium set* $E_P(f)$ as the subset of the configuration space $\mathcal{C}$ for which P is in equilibrium. Let us write $f * g$ for a strategy that first applies vector field f, and then vector field g to move part P. $f + g$ can be understood as applying f and g simultaneously. We have shown that in general $E_P(f)$ is not finite, but for two *orthogonal* squeezes f and g, the discrete switching strategy $f * g$ yields a finite equilibrium set $E_P(f * g)$ (see Section 6.2, Claim 28). Furthermore, for some parts the equilibrium is unique up to symmetry.

We wish to explore the relationship between equilibria in simple vector fields $E_P(f)$ or $E_P(g)$, combined fields $E_P(f + g)$, discretely-switched fields $E_P(f * g)$, and continuously varying fields $E_P(f \rightsquigarrow g)$. For example, one may ask whether there exists a strategy with combined vector fields, or continuously varying fields, that, in just one step, reaches the same equilibrium as a discretely switched strategy requiring multiple steps. Finally, let $f_1 * f_2 * \cdots * f_s$ be a sequence of squeeze fields guaranteed to uniquely orient a part P under assumption 2PHASE. We wish to investigate how continuously varying strategies such as $f_1 \rightsquigarrow f_2 \rightsquigarrow \cdots \rightsquigarrow f_s$ can be employed to dynamically achieve the same equilibria even when 2PHASE is relaxed. The distributed actuation strategy $F * G$ is distributed in space, but not in time. The strategy $F + G$ is parallel with respect to space and time, since F and G are simultaneously "run." Research in this area could lead to a *theory of parallel distributed manipulation* that describes *spatially distributed* manipulation tasks that can be *parallelized over time and space* by superposition of controls.

5.2 Upward-Shaped Potential Fields

So far we have presented specific force fields that *always* (e.g. squeeze and radial fields) or *never* (e.g. skewed squeeze fields) induce stable equilibria on certain classes of parts. We conclude this section with a criterion that provides a sufficient condition on force fields such that *all parts of a certain size reach a stable equilibrium.*

We have observed in Section 4 that *a priori* it is not obvious when a force field induces stable equilibria. Our Equilibrium Criterion will be based on two important properties:

1. The field has a potential. Potential fields do not allow closed paths (technically, limit cycles) along which the work is positive, which could induce infinite motion of a part.
2. The force field is "inward-directed," which implies that (assuming first-order dynamics) parts can never leave a certain region R. This useful property is a direct consequence of the definition of inward-directedness. An inward-directed force field corresponds to an "upward-shaped" potential, in which all paths that leave region R have an ascending slope.

We will require Property (1.) to hold for the entire force field, while Property (2.) devolves to a boundary condition.

5.2.1 Elementary Definitions

Definition 16 *Let* $\mathbf{z} \in \mathbb{R}^n$. *The* ϵ-ball around $\mathbf{z}$, *denoted* $B_\epsilon(\mathbf{z})$, *is the set* $\{\mathbf{r} \in \mathbb{R}^n \mid |\mathbf{r} - \mathbf{z}| < \epsilon\}$ *of all points within a distance* ϵ *of* $\mathbf{z}$.

Definition 17 (Lozano-Pérez [32]) *Let* A, B *be sets in* $\mathbb{R}^n$. *The* Minkowski sum $A \oplus B$ *of two sets* A *and* B *is defined as the set* $\{\mathbf{a} + \mathbf{b} \mid \mathbf{a} \in A, \mathbf{b} \in B\}$.

From these definitions it follows that for a region R with boundary ∂R, the set $\partial R \oplus B_d(\mathbf{0}) = \{\mathbf{r} + \mathbf{z} \mid \mathbf{r} \in \partial R, \text{ and } |\mathbf{z}| \leq d\}$ comprises all points that are within a distance d from the boundary of R.

Definition 18 *Given a region* $R \subset \mathbb{R}^n$, *define the set* $CI(R,d) = R - (\partial R \oplus B_d(\mathbf{0}))$ *which is the region* R *shrunk by distance* d. *Note that* $CI(R,d)$ *is based upon the* configuration space interior [32] *of* R *for* $B_d(\mathbf{0})$. *Abusing terminology slightly, we call* $CI(R,d)$ *the* configuration space interior of R *in this paper.*

Definition 19 *The* radius r_P of a part P *is the maximum distance between an arbitrary point of* P *and the center of mass (COM) of* P.

5.2.2 Equilibrium Criterion

We are now able to state a general criterion for a force field f to induce stable equilibria on all parts in a region S. As mentioned at the beginning of Section 5.2, this criterion is based on two main conditions: (1) if f has a potential, limit cycles with positive energy gain are avoided inside S. (2) if f is "inward-directed" (see the definition below), parts cannot leave the region S.

In the following we give a general definition of inward-directed vector fields on a manifold Z. We then specialize the definition to the special instances of $Z = \mathcal{C} = \mathbb{R}^2 \times \mathbb{S}^1$ (the configuration space) and $Z = \mathbb{R}^2$, and give a sufficient, practical condition for inward-directed vector fields. We conclude with the presentation of the Equilibrium Criterion.

Definition 20 (Inward-Directed Force Fields) [3] *Let Z be an arbitrary smooth manifold, and let $Y \subset Z$ be a compact and smooth submanifold with boundary of Z. Assume that ∂Y has codimension 1 in Z, and that the boundary of Y is orientable. Let $q \in \partial Y$ be a point on the boundary of Y, and $V_q \in T_q Z$ be a tangent vector to Z at q.*

We say V_q is inward-directed to ∂Y at q *if there exists a sufficiently small $\epsilon > 0$ such that $q + \epsilon V_q \in Y$.*

Let V be a vector field on Z. We say V is inward-directed to ∂Y *if $V(q)$ is inward-directed to ∂Y at q for all $q \in \partial Y$.*

Assume the set $S \subset \mathbb{R}^2$ is compact and smooth. Consider the part P when it is placed into the force field f such that its COM lies in S. The set of all such poses is a subset of the configuration space $\mathcal{C} = \mathbb{R}^2 \times \mathbb{S}^1$ which we call $\widetilde{S} = S \times \mathbb{S}^1$. The boundary of $\widetilde{S}$ is $\partial\widetilde{S} = \partial S \times \mathbb{S}^1$. Note that $\partial\widetilde{S}$ separates the interior $i\widetilde{S} = \widetilde{S} - \partial\widetilde{S}$ from the exterior $\mathcal{C} - \widetilde{S} = (\mathbb{R}^2 - S) \times \mathbb{S}^1$, and that $\partial\widetilde{S}$ is isomorphic to a torus $\mathbb{S}^1 \times \mathbb{S}^1$.

Now let $z = (x, y, \theta) \in \partial\widetilde{S}$, and let $F_z \in T_z\mathcal{C}$ represent the lifted generalized force acting on part P in pose z. F_z is *inward-directed* (w.r.t. $\partial\widetilde{S}$) if F_z points into the interior of $\widetilde{S}$. Note that this condition is equivalent to saying that the projection of F_z onto the tangent space at (x, y) to $\mathbb{R}^2$ points into S, because the rotational component of F_z is tangential to $\partial\widetilde{S}$. So for example, if $z = (x, y, \theta) \in \partial\widetilde{S}$, then $z' = (x, y, \theta') \in \partial\widetilde{S}$ for any θ'.

The following proposition gives a simple condition on a force field f that tells us if, for a given part P, its lifted generalized force field F_P is inward-directed:

Proposition 21 *Let P be a part with radius r whose COM is the reference point used to define its configuration space $\mathcal{C} = \mathbb{R}^2 \times \mathbb{S}^1$. Let f be a force vector field defined on a region $R \subset \mathbb{R}^2$, with F_P the corresponding lifted generalized force field. Let $S \subset \mathbb{R}^2$ be a convex, compact, and smooth subset of the configuration space interior of R, and $S \subset CI(R, r)$.*

Consider a point $q \in \partial S$ with outward normal n_q, and a ball $B_r(q)$ with radius r about q. If for every point $q \in \partial S$, and for every point s in the corresponding ball $B_r(q)$, the dot product $g(s) = f(s) \cdot n_q$ is less than 0, then the lifted generalized force field F_P is inward-directed to $\partial\widetilde{S}$ (note: $(\cdot)$ is the standard inner product).

Proof: Consider the part P in pose $z = (x, y, \theta) \in \partial\widetilde{S}$ such that $q = (x, y)$. P has radius r, hence it lies completely inside the ball $B_r(q)$, independent of its orientation θ. As we know that $g(p) = f(p) \cdot n_q < 0$ for all $p \in B_r(q)$, we can conclude that the integral of $g(p)$ over P is also less than 0: $\int_P g(p)\, dA = \int_P f(p) \cdot n_q\, dA = f_P \cdot n_q < 0$. This implies that for f_P, which is the translational component of F_P (see Definition 14), the vector $q + \epsilon\, f_P(z)$ lies inside S, if ϵ is positive and sufficiently small. As mentioned above in Section 5.2.2, this suffices to ensure that the vector $z + \epsilon\, F_P(z)$ lies inside $\widetilde{S}$. □

Lemma 22 (Equilibrium Criterion) *Let P be a part with radius r, let f be a force field with potential U defined on a region $R \subset \mathbb{R}^2$, and let $S \subset R$ as specified in Proposition 21. Let us also assume that the motion of part P is governed by first-order dynamics.*

If the lifted force vector field F_P is inward-directed to $\partial\widetilde{S}$, then the part P will reach a stable equilibrium under f in $i\widetilde{S}$ whenever its COM is initially placed in S.

Proof: Assume that the COM of part P is placed at a point $(x, y) \in S$. This means that P is in some pose $z = (x, y, \theta) \in \widetilde{S}$. We now show that the COM of

[3] In this definition, for convenience we assume that Z is embedded in $\mathbb{R}^m$ for some m. This condition may be relaxed.

P cannot leave S when initially placed inside S. We know that $\partial\widetilde{S}$ separates $i\widetilde{S}$ from $\mathcal{C} - \widetilde{S}$. Hence every path from z to some $z^* \in \mathcal{C} - \widetilde{S}$ must intersect $\partial\widetilde{S}$ at some point $z' \in \partial\widetilde{S}$. Now consider part P in pose z'. Under first-order dynamics, its velocity must be in direction of $F_P(z')$. Because F_P is inward-directed, the velocity of P must be towards $i\widetilde{S}$. In particular, this means that the COM will move into iS, hence P cannot leave S, and that there is no equilibrium on ∂S.

f, and hence (because of Proposition 15) F_P have potential U and U_P, respectively. Therefore limit cycles with energy gain are not possible. Furthermore, $U_P(\widetilde{S})$ is the continuous image of a compact set, $\widetilde{S}$. Therefore the image $U_P(\widetilde{S})$ is a compact subset of $\mathbb{R}$, hence has a minimum value attained by some point $s \in \widetilde{S}$. Since f is inward-directed, s must lie in $i\widetilde{S}$. This minimum is a stable equilibrium of P in f. □

Because of Lemma 22, the use of potential fields is invaluable for the analysis of effective and efficient manipulation strategies, as discussed in the following section. In particular, it is useful for proving the completeness of a manipulation planner.

6 New and Improved Manipulation Algorithms

The part alignment strategies in Section 3.2 have *switch points* in time where the vector field changes discontinuously (Figure 5). We can denote such a *switched strategy* by $f_1 * f_2 * \cdots * f_s$, where the f_i are vector fields. In Section 3.2 we recalled that a strategy to align a (non-convex) polygonal part with n vertices may need up to $O(k\,n^2)$ switches, and require $O(k^2\,n^4)$ time in planning (k is the maximum number of polygon edges that a bisector can cross). To improve these bounds, we now consider a broader class of vector fields including simple squeeze patterns, radial, and combined fields as described in Section 5.

In Section 6.1 we show how, by using radial and combined vector fields, we can significantly reduce the complexity of the strategies from that of Section 3. In Section 6.2 we describe a general planning algorithm that works with a limited "grammar" of vector fields (and yields, correspondingly, less favorable complexity bounds).

6.1 Radial Strategies

Consider a part P in a force field f. Some force fields exhibit rotational symmetry properties that can be used to generate efficient manipulation strategies:

Property 23 *There exists a unique* pivot point v *of* P *such that* P *is in translational equilibrium if and only if* v *coincides with* $\mathbf{0}$.

Property 24 *There exists a unique* pivot point v *of* P *such that* P *is in (neutrally stable) orientational equilibrium if and only if* v *coincides with* $\mathbf{0}$.

We typically think of the pivot point v being a point of P; however, in generality, just like the center of mass of P, v does not need to lie within P, but instead is some fixed point relative to the reference frame of P. Now consider the part P in an ideal unit radial force vector field R as described in Section 5.

Proposition 25 *In a unit radial field* R, *Properties 23 and 24 hold.*

Proof: We fix the part P at an arbitrary orientation θ, and show that at this orientation P has a unique translational equilibrium $v(\theta)$. That is, placing $v(\theta)$ at the origin is necessary and sufficient for P to be in translational equilibrium at orientation θ. Second, we show that for any two distinct orientations θ and θ', $v(\theta) = v(\theta')$. We call this unique point v, dropping the orientation θ. Finally, we argue that whenever P is in translational equilibrium (i.e., v is at the origin), that P is neutrally stable w.r.t. orientation. This follows by the radial symmetry of R.

Consider the translational forces (but not the moments) acting on P in the radial field R. To do this, let us separate R into its x and y components, R_x and R_y, such that $R = (R_x, R_y)$. Assume for now that the orientation of P is fixed. If P is placed at a position $z_0 \in \mathbb{R}^2$, whose x-coordinate is sufficiently negative, the total force induced by R_x on P will point in the positive x direction. Symmetrically, placing P at a sufficiently large positive x coordinate will cause a force in the negative x direction. We claim that, by translating P rigidly with increasing x coordinate, this force decreases continuously and strictly monotonically, and hence has a unique root.

To verify this claim, consider a small area patch $\wp_0$ of P. A uniform translation t of $\wp_0$ in x direction can

be described as $\wp(t) = \wp_0 \oplus (z_0 + t\hat{x})$ (with z_0 the initial position of the patch, $\hat{x}$ the unit vector in x direction, and $\oplus$ the Minkowski sum). The total force on $\wp(t)$ in x direction is $\int_{\wp(t)} R_x \; dA$. This force decreases continuously and strictly monotonically with t, because R_x is strictly monotone and continuous everywhere except on the x-axis, which has measure zero in $\mathbb{R}^2$. A similar argument applies for the y direction, and, because of the radial symmetry of R, for any direction.

If we choose the set S as a sufficiently large disk-shaped region around the origin and recall that R has a potential, we can apply Lemma 22 to conclude that there must exist at least one total equilibrium for P. Now assume that there exist two distinct equilibria $e_1 = (x_1, y_1, \theta_1)$ and $e_2 = (x_2, y_2, \theta_2)$ for P in R. We write "$P(e_i)$" to denote that P is in configuration e_i. Because of the radial symmetry of R, we can reorient $P(e_2)$ to $P(e_2')$ such that its orientation is equal to $P(e_1)$: $e_2' = (x_2', y_2', \theta_1)$, where $\binom{x_2'}{y_2'} = M \binom{x_2}{y_2}$, and M is a rotation matrix with angle $\theta_1 - \theta_2$. This reorientation does not affect the equilibrium. Note that P can be moved from e_1 to e_2' by a pure translation. From above we know that such a translation of P corresponds to a strictly monotone change in the translational forces acting on P. Hence we conclude that $P(e_1)$ and $P(e_2')$ cannot both be in translational equilibrium unless e_1 and e_2' are equal. This implies that e_1 and e_2 cannot both be equilibria of P in R unless they both have the same pivot point v. □

Surprisingly, v need not be the center of area of P. For example, consider a large and a small square connected by a long rod of negligible width. The pivot point of this part will lie inside the larger square. But if the rod is long enough, the center of area will lie outside of the larger square. However, the following corollary holds:

Corollary 26 *For a part P in a continuous radial force field R' given by $R'(\mathbf{z}) = -\mathbf{z}$, the pivot point of P coincides with the center of area of P.*

Proof: The force acting on P in R' is given by $F = \int_P -\mathbf{z} \; dA$, which is also the formula for the (negated) center of area. □

Now suppose that R is combined with a unit squeeze pattern S, which is scaled by a factor $\delta > 0$, resulting in $R + \delta S$. The squeeze component δS of this field will cause the part to align with the squeeze, similarly to the strategies in Section 3.2. But note that the radial component R keeps the part centered in the force field. Hence, by keeping R sufficiently large (or δ small), we can assume that the pivot point of P remains within an ϵ-ball of the center of R. This implies that assumption 2PHASE (see Section 3.2) is no longer necessary. Moreover, ϵ can be made arbitrarily small by an appropriate choice of δ.

Proposition 27 *Let P be a polygonal part with n vertices, and let k be the maximum number of edges that a bisector of P can cross. Let us assume that v, the pivot point of P, is in general position. There are at most $O(k\,n)$ stable equilibria in a field of the form $R + \delta S$ if δ is sufficiently small and positive.*

Proof: For a part in equilibrium in a pure radial field R (i.e., with $\delta = 0$), the pivot point v is essentially fixed at the origin. This is implied by Property 23. It is easy to see that Property 23 is not true in general for arbitrary fields of the form $R + \delta S$. Property 23 holds if $\delta = 0$, because then any orientation is an equilibrium when v is at the center of R. However, Property 24 does not hold if $\delta > 0$, because in general there does not exist a unique pivot point in squeeze fields (see Section 3.2).

We will conduct the combinatorial analysis of the orientation equilibria under the assumptions that (i) $\delta > 0$ and (ii) that v is fixed at the origin. Then we will relax the latter assumption (ii), and show that Property 23 holds, *approximately,* even in $R + \delta S$, for a sufficiently small $\delta > 0$. That is, we show that a sufficiently small δ can be chosen so that the combinatorial analysis is unaffected when assumption (ii) is relaxed.

First, we show that when δ is small but positive, and with v fixed at the center of R, there are only a linear number of orientation equilibria. (I.e., we constrain the pivot point v to remain fixed at the origin until further notice.) So let us assume that we are in a combined radial and small squeeze field $R + \delta S$.

Consider a ray $w(0)$ emanating from v. Assume w.l.o.g. that v is not a vertex of P, and that $w(0)$ intersects the edges $S(0) = \{e_1, \cdots, e_k\}$ of P in general position, $1 \leq k \leq n$. Parameterize the ray $w(\cdot)$ by its angle ϕ to obtain $w(\phi)$. As ϕ sweeps from 0 to 2π, each edge of P will enter and leave the *crossing*

structure $S(\phi)$ exactly once. $S(\phi)$ is updated at *critical angles* where $w(\phi)$ intersects a vertex of P. Since there are n vertices, there are $O(n)$ critical angles, and hence $O(n)$ changes to $S(\phi)$ overall. Hence, since between critical angles $S(\phi)$ is constant, we see that $S(\phi)$ takes on $O(n)$ distinct values. Now place the squeeze line l to coincide with $w(\phi)$. For a given crossing structure $S(\phi) \cup S(\phi + \pi)$, satisfying conditions **I** and **II** as defined in Section 3.2 devolves to solving two algebraic equations of degree k, where k is the maximum number of edges intersected by the squeeze line as described in Section 3.1. This implies that between any two adjacent critical values there are only $O(k)$ orientations of l (given by $w(\phi)$) that satisfy conditions **I** and **II**. Hence, the overall number of orientations satisfying **I** and **II** is $O(k\,n)$.

If $\delta > 0$ the part P will be perturbed, so that Property 23 is only approximately satisfied. (That is, we now relax the assumption that v is constrained to be at the origin). However, we can ensure that v lies within an ϵ-ball around the origin (the center of the radial field). To see this, first consider P at some arbitrary configuration $\mathbf{z}$ in the squeeze field δS. The total squeeze force on $P_{\mathbf{z}}$ is given by the area integral $\delta S_P(\mathbf{z}) = \int_{P_{\mathbf{z}}} \delta S \, dA$. (Recall that S_P denotes the lifted force field of S; see Definition 14, Equation (2).) Now, δS_P is bounded above by $|\delta S_P| \leq \delta A$, where A is the area of P (note that S is a unit squeeze field).

P is in equilibrium with respect to the radial field R if v is at the origin. Now consider the lifted force R_P when the pivot point of P is not at the origin. More specifically, Let $v_{\mathbf{z}}$ be the pivot point of $P_{\mathbf{z}}$, and let us define a function $\widehat{R}_P(d) = \min\{|R_P(\mathbf{z})| \text{ such that } |v_{\mathbf{z}}| = d\}$, i.e., $\widehat{R}_P(d)$ is the minimum magnitude of the lifted force acting on $P_{\mathbf{z}}$ when its pivot point $v_{\mathbf{z}}$ is at distance d from the origin.

By decomposing R_P into its x- and y-components, we can write $|R_P|$ as $\sqrt{R_{P,x}^2 + R_{P,y}^2}$. Because of the radial symmetry of R let us assume w.l.o.g. that $v_{\mathbf{z}} = (d, 0)$. From the proof of Proposition 25 we know that, for any given orientation of $P_{\mathbf{z}}$, the magnitude of $R_{P,x}$ increases continuously and strictly monotonically with increasing $d \geq 0$. Furthermore, $R_{P,y}$ is continuous in d, and $R_{P,y}(\mathbf{0}) = 0$, so $R_{P,y}^2$ is continuous and monotonically increasing for all d less than some sufficiently small $d_0 > 0$. Hence for any fixed orientation of $P_{\mathbf{z}}$, R_P is a continuous and strictly monotonically increasing function for all $d \in [0, d_0]$. This implies that $\widehat{R}_P$ is also continuous and strictly monotone for sufficiently small $d \geq 0$.

Now consider $P_{\mathbf{z}}$ in equilibrium in the combined field $R + \delta S$, and again let d denote the distance between pivot point $v_{\mathbf{z}}$ and the origin. In equilibrium the lifted forces R_P and δS_P balance out, hence $\widehat{R}_P(d) \leq |R_P| = |\delta S_P| \leq \delta A$. Since $\widehat{R}_P$ is continuous and strictly monotone in d for sufficiently small d, we can ensure that d is less than a given ϵ, by chosing an appropriately small δ. This implies that $v_{\mathbf{z}}$ must lie within an ϵ-ball of the center of the radial field. In particular, we can make this ϵ-ball small enough so that the crossing structure $S(\phi)$ is not affected. Keeping d small also ensures that the torque τ_R about the pivot point induced by the radial field R is small, because τ_R is bounded by the product of d and R_P. This ensures that the equilibria of the squeeze field δS are not affected.

We conclude that the number of equilibria in a field $R + \delta S$ is bounded by $O(k\,n)$, for sufficiently small δ. □

In analogy to Section 3.2 we define the turn function $t : \mathbb{S}^1 \to \mathbb{S}^1$, which describes how the part will turn under a squeeze pattern, and hence yields the stable equilibrium configurations. Given the turn function t we can construct the corresponding squeeze function s as described in Section 3.2. With s as the input for Goldberg's alignment planner, we obtain strategies for unique part alignment (and positioning) of length $O(k\,n)$. They can be computed in time $O(k^2\,n^2)$.

The result is a strategy for parts positioning of the form $(R + \delta S_1) \ * \cdots * \ (R + \delta S_{O(kn)})$. Compared to the old algorithm in Section 3.2 it improves the plan length by a factor of n, and the planning complexity is reduced by a factor of n^2. The planner is complete: For any polygonal part, there exists a strategy of the form $*_i(R + \delta S_i)$. Moreover, the algorithm is guaranteed to find a strategy for any input part. By appending a step which is merely the radial field R without a squeeze component, we are guaranteed that the part P will be uniquely posed (v is at the origin) as well as uniquely oriented. We can also show that the continuously varying "morphing" strategy $(R+\delta S_1) \rightsquigarrow \cdots \rightsquigarrow (R+\delta S_{O(kn)}) \rightsquigarrow R$ works in the same fashion to achieve the same unique equilibrium.

6.2 Manipulation Grammars

The development of devices that generate programmable vector fields is still in its infancy. The existing prototype devices exhibit only a limited range of programmability. For example, the prototype MEMS arrays described in Section 2.1 [9, 8, 7] currently have actuators in only four different directions, and the actuators are only row-wise controllable. Arrays with individually addressable actuators at various orientations are possible (see [9, 8, 31, 7, 42]) but require significant development effort. There are also limitations on the resolution of the devices given by fabrication constraints. For the vibrating plate device from Section 2.2 the fields are even more constrained by the vibrational modes of the plate.

We are interested in the capabilities of such constrained systems. In this section we give an algorithm that decides whether a part can be uniquely positioned using a given set of vector fields, and it synthesizes an optimal-length strategy if one exists. If we think of these vector fields as a vocabulary, we obtain a language of manipulation strategies. We are interested in those expressions in the language that correspond to a strategy for uniquely posing the part.

The elements of our "manipulation grammar" are (sequences of) vector fields that bring the part into a *finite* set of possible equilibrium positions (Figure 8). We call these (sequences of) vector fields *finite field operators*. Each field operator comes with the following guarantee: No matter where in $\mathbb{R}^2 \times \mathbb{S}^1$ the part starts off, it will always come to rest in one of E different total equilibria. That is: For any connected polygonal part P, either of these field operators is *always* guaranteed to reduce P to a *finite* set of equilibria in its configuration space $\mathcal{C} = \mathbb{R}^2 \times \mathbb{S}^1$.

From Section 6.1 we know that combined radial-squeeze patterns $R + \delta S$ have this property. However, there are other simple field operators that also have this finiteness property:

Claim 28 *Let f and $f_\perp$ be unit squeeze fields such that $f_\perp$ is orthogonal to f. Then the fields $f * f_\perp$ and $f + f_\perp$ induce a finite number of equilibria on every connected polygon P.*

Proof: First consider the field $f * f_\perp$, and w.l.o.g. assume that $f(x, y) = (-\text{sign}(x), 0)$. Also assume that

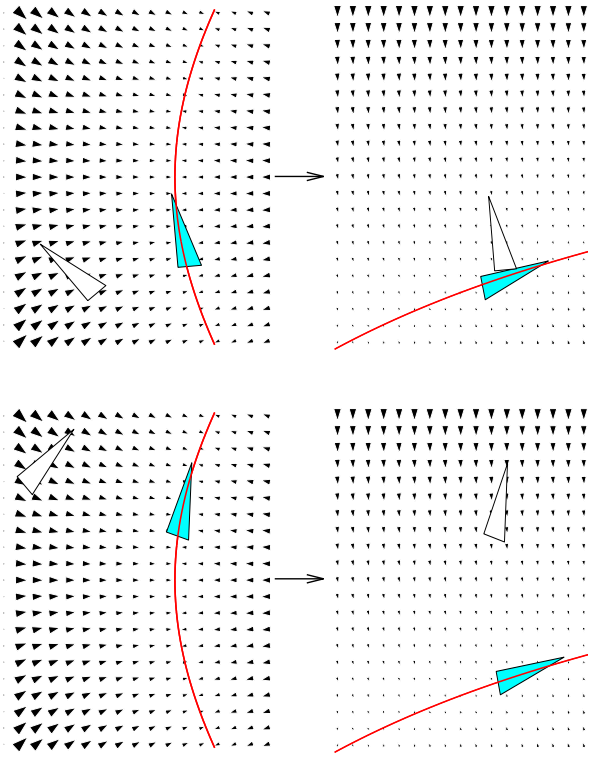

Figure 8: *Alignment vocabulary for a triangular part on a vibrating plate, consisting of two consecutive force fields with slightly curved nodal lines (attractors) which bring the part into (approximately) the same equilibria.*

the COM of P is the reference point used to define its configuration space $\mathcal{C} = \mathbb{R}^2 \times \mathbb{S}^1$. As discussed in Section 3.1, P will reach one of a finite number of orientation equilibria when placed in f or $f_\perp$. More specifically, when P is placed in f, there exists a finite set of equilibria $E_f = \{(x_i, \theta_i)\}$. Similarly for $f_\perp(x, y) = (0, -\text{sign}(y))$, there exists a finite set of equilibria $E_{f_\perp} = \{(y_j, \theta_j)\}$. Since the x-component of $f_\perp$ is zero, the x-coordinate of the reference point of P (the COM) remains constant while P is in $f_\perp$. Hence P will finally come to rest in a pose (x_k, y_k, θ_k), where $x_k \in \pi_1(E_f)$, $(y_k, \theta_k) \in E_{f_\perp}$, and π_1 is the canonical projection such that $\pi_1(x, y, \theta) = x$. Since E_f is finite, so is $\pi_1(E_f)$. $E(f_\perp)$ is also finite, therefore there exists only a finite number of such total equilibrium poses for $f * f_\perp$.

If P is placed into the field $f + f_\perp$, there exists a

unique translational equilibrium (x, y) for every given, fixed orientation θ. In each of these translational equilibria, the squeeze lines of f and $f_\perp$ are both bisectors of P. Now consider the moment acting on P when P is in translational equilibrium as a function of θ. In analogy to Proposition 4 in Section 3.1 we can show that for any topological placement of the bisectors, this moment function has at most $O(k)$ roots, where k is the maximum number of edges a bisector of P can cross. This implies that there exist only $O(k\,n^2)$ distinct total equilibria for $f + f_\perp$. □

We have seen in Sections 3 and 5 that for simple force fields such as e.g. squeeze or radial fields, we can predict the motion and the equilibria of a part with exact analytical methods. However, for arbitrary fields (e.g. the force fields described in Section 2.2 which are induced by vibrating plates) such algorithms may not exist. Instead we can employ approximate methods to predict the behavior of the part in the force field (for more details also see [18]). These methods are typically numerical computations that involve simulating the part from a specific initial pose, until it reaches equilibrium.[4] We call the cost for such a computation the *simulation complexity* $s(n)$. We write $s(n)$ because the simulation complexity will usually depend on the complexity of the part (i.e. its number of vertices n).

Proposition 29 *Consider a polygonal part P, and m finite field operators $\{F_i\}$, $1 \le i \le m$, each with at most E distinct equilibria in the configuration space $\mathcal{C}$ for P. There is an algorithm that generates an optimal-length strategy of the form $F_1 * F_2 * \cdots * F_m$ to uniquely pose P up to symmetries, if such a strategy exists. This algorithm runs in $O(m^2 E\ (s(n)+2^E))$ time, where $s(n)$ is the simulation complexity of P in F_i. If no such strategy exists, the algorithm will signal failure.*

Proof: Construct a transition table T of size $m^2 E$ that describes how the part P moves from an equilibrium of F_i to an equilibrium of F_j. This table can be constructed either by a dynamical analysis similar to Section 6.1, or by dynamic simulation. The time to construct this table is $O(m^2 E\ s(n))$, where $s(n)$ is the simulation complexity, which will typically depend on the complexity of the part.

[4] See for example URL `http://www.cs.cornell.edu/home/karl/Cinema`.

Using the table T, we can search for a strategy as follows: Define the *state* of the system as the set of possible equilibria a part is in, for a particular finite field operator F_i. There are m field operators and $O(E)$ equilibria for each of them, hence there are $O(m\ 2^E)$ distinct states. For each state there are m possible successor states as given by table T, and they can each be determined in $O(E)$ operations, which results in a graph with $O(m\ 2^E)$ nodes, $O(m^2\ 2^E)$ edges, and $O(m^2 E\ 2^E)$ operations for its construction. Finding a strategy, or deciding that it exists, then devolves to finding a path whose goal node is a state with a unique equilibrium. The total running time of this algorithm is $O(m^2 E\ (s(n) + 2^E))$. □

Hence, as in [21], for any part we can decide whether a part can be uniquely posed using the vocabulary of field operators $\{F_i\}$ but (a) the planning time is exponential and (b) we do not know how to characterize the class of parts that can be oriented by $\{F_i\}$. However, the resulting strategies are optimal in size.

This result illustrates a tradeoff between mechanical complexity (the dexterity and controllability of field elements) and planning complexity (the computational difficulty of synthesizing a strategy). If one is willing to build a device capable of radial fields, then one reaps great benefits in planning and execution speed. On the other hand, we can still plan for simpler devices (see Figures 3 and 8), but the plan synthesis is more expensive, and we lose some completeness properties.

7 Conclusions and Open Problems

Universal Feeder-Orienter (UFO) Devices. It was shown in [8] that every connected polygonal part P with n vertices has a finite number of stable orientation equilibria when P is placed into a squeeze field S. Based on this property we were able to generate manipulation strategies for unique part alignment. We showed in Section 6.1 that by using a combined radial and squeeze field $R + \delta S$, the number of equilibria can be reduced to $O(k\,n)$. Using elliptic force fields $f(x, y) = (\alpha x, \beta y)$ such that $\alpha \neq \beta$ and $\alpha, \beta \neq 0$, this bound can be reduced to 2 [29]. Does there exist a *universal field* that, for every part P, has only one unique equilibrium (up to part symmetry)? Such a field could be used to build a *universal parts feeder* [1]

that uniquely positions a part without the need of a clock, sensors, or programming.

We propose a combined radial and "gravitational" field $R + \delta G$ which might have this property. δ is a small positive constant, and G is defined as $G(x, y) = (0, -1)$. This device design is inspired by the "universal gripper in [1]. Such a field could be obtained from a MEMS array that implements a unit radial force field. Instead of rectangular actuators in a regular grid, triangular actuators could be laid out in a polar-coordinate grid. The array could then be tilted slightly to obtain the gravity component. Hence such a device would be relatively easy to build. Extensive simulations show that for every part we have tried, one unique total equilibrium is always obtained. We are working toward a rigorous proof of this experimental observation.

Magnitude Control. Consider an array in which the *magnitude* of the actuator forces cannot be controlled. Does there exist an array with constant magnitude in which all parts reach one unique equilibrium? Or can one prove that, without magnitude control, the number of distinct equilibria is always greater than one?

Geometric Filters. This paper focuses mainly on sensorless manipulation strategies for *unique positioning* of parts. Another important application of programmable vector fields are *geometric filters*. Figure 1 shows a simple filter that separates smaller and larger parts. We are interested in the question *Given n parts, does there exist a vector field that will separate them into specific equivalence classes?* For example, does there exist a field that moves small and large rectangles to the left, and triangles to the right? In particular, it would be interesting to know whether for any two different parts there exists a sequence of force fields that will separate them.

Performance Measures. Are there performance measures for how fast (in real time) an array will orient a part? In some sense the actuators are fighting each other (as we have observed experimentally) when the part approaches equilibrium. For squeeze grasps, one measure of "efficiency", albeit crude, might be the integral of the magnitude of the moment function, i.e., $\int_0^{2\pi} |M(\theta)|\, d\theta$. The issue is that if, for many poses, $|M(\theta)|$ is very small, then the orientation process will be slow. Better measures are also desirable.

Uncertainty. In practice, neither the force vector field nor the part geometry will be exact, and both can only be characterized up to tolerances [15]. This is particularly important at micro scale. Within the framework of potential fields, we can express this uncertainty by considering not one single potential function U_P, but rather *families of potentials* that correspond to different values within the uncertainty range. Bounds on part and force tolerances will correspond to limits on the variation within these function families. An investigation of these limits will allow us to obtain upper error bounds for manipulation tasks under which a specific strategy will still achieve its goal.

A family of potential functions is a set $\{U_\alpha : \mathcal{C} \to \mathbb{R}\}_{\alpha \in J}$ where J is an index set. For example, we may start with a single potential function $U : \mathcal{C} \to \mathbb{R}$, and define a family of potential functions $\mathcal{F}(U, \epsilon, z)$ as $\{U_\alpha : \mathcal{C} \to \mathbb{R} \mid \|U_\alpha(p) - U(p)\|_z < \epsilon\}$ for some ϵ and norm z. This is analogous to defining a neighborhood in function space, using e.g. the compact-open topology.

When we differentiate a family of potential fields (using the gradient) we obtain a differential inclusion instead of a differential equation. So if $\mathcal{F}(u) = \mathcal{F}(u, \epsilon, z)$, then $\nabla\mathcal{F}(u) = \{\nabla U_\alpha\}_{\alpha \in J}$.

When considering families of potentials, the equilibrium may be known to lie only within a set E_i, although we may know that it is always a point in E_i. If the sets E_i are of a small diameter less than some $\epsilon > 0$, our algorithms could be extended to handle ϵ-approximations.

As a more general approach, we propose an algorithm based on *back-projections*: For a given part, let $B_{F_i}(G) \subset \mathcal{C} = \mathbb{R}^2 \times \mathbb{S}^1$ be the back-projection [33] of the set G under F_i, where $G \subset \mathcal{C}$, and F_i is a family of fields on $\mathbb{R}^2$. Then we wish to calculate a sequence of fields $F_1, F_2, \cdots, F_k$ such that $B_{F_1}(B_{F_2}(\cdots B_{F_k}(G)\cdots)) = \mathcal{C}$, where G is a single point in $\mathcal{C}$ (cf. [33, 21, 13, 15, 11]).

Output Sensitivity. We have seen in Sections 6.1 and 6.2 that the efficiency of planning and executing manipulation strategies critically depends on the number of equilibrium configurations. Expressing the planning and execution complexity as a function of the

number of equilibria E, rather than the number of vertices n, is called *output sensitive analysis*. In practice, we have found that there are almost no parts with more than two distinct (orientation) equilibria, even in squeeze fields. This is far less than the $E = O(k\,n^2)$ upper bound derived in 3.1. If this observation can be supported by an exact or even statistical analysis of part shapes, it could lead to extremely good expected bounds on plan length and planning time, even for the less powerful strategies employing manipulation grammars (note that the complexity of the manipulation grammar algorithm in Proposition 29 is output-sensitive).

Discrete Force Fields. For the manipulation strategies described in this paper we assume that the force fields are continuous, i.e. that the generated forces are dense compared to the moving part (assumption DENSITY in Section 3.2). When manipulating very small parts on microactuator arrays, this condition may be only approximately satisfied. We are interested in the limitations of the continuous model, and we would like to know the conditions under which it is necessary to employ a different, discrete model of the array that takes into account individual actuators, as well as the gaps between actuators. In [9] we propose a model for the interaction between parts and arrays of individual actuators based on the theory of limit surfaces [26].

Resonance Properties. Is it possible to exploit the dynamic resonance properties of parts to tune the AC control of the array to perform efficient dynamic manipulation?

3D Force Fields. It may be possible to generate 3D force fields by using Lorentz electromagnetic forces. Tunable electric coils could be attached to various points of a 3D body, suspending the resulting object in a strong permanent magnetic field using magnetic levitation (the Lorentz effect) [28]. The tuning (control) of the electric coils could be effected as follows: Integrated control circuitry could be fabricated and co-located with the coils, and conceivably a power supply. The control could be globally effected using wireless communication, or, the control of each coil evolves in time until the part is reoriented as desired. The Lorentz forces could then be deactivated to bring the object to rest on the ground. Planning for such a 3D device might reduce to [23].

Acknowledgments

We would like to thank Tamara Lynn Abell, Vivek Bhatt, Bernard Chazelle, Paul Chew, Perry Cook, Ivelisse Rubio, Ken Steiglitz, Nick Trefethen, and Andy Yao for useful discussions and valuable comments. We are particularly grateful to Mike Erdmann for his suggestions and help for the proofs of Proposition 15 and Lemma 22, to Danny Halperin for sharing his insights into geometric and topological issues related to manipulation with force fields, to Lydia Kavraki for continuing discussions and creative new ideas concerning force vector fields, and Jean-Claude Latombe for his hospitality during our stay at the Stanford Robotics Laboratory.

Support is provided in part by the NSF under grants No. IRI-8802390, IRI-9000532, IRI-9201699, and by a Presidential Young Investigator award to Bruce Donald, in part by NSF/ARPA Special Grant for Experimental Research No. IRI-9403903, and in part by the AFOSR, the Mathematical Sciences Institute, Intel Corporation, and AT&T Bell laboratories. This work was supported by ARPA under contract DABT 63-69-C-0019. The device fabrication was performed at the Cornell Nanofabrication Facility (CNF), which is supported by NSF grant ECS-8619049, Cornell University, and Industrial Affiliates.

References

[1] T. L. Abell and M. Erdmann. A universal parts feeder, 1996. Personal communication / in preparation.

[2] S. Akella, W. H. Huang, K. M. Lynch, and M. T. Mason. Planar manipulation on a conveyor by a one joint robot with and without sensing. In *International Symposium of Robotics Research (ISRR)*, 1995.

[3] K.-F. Böhringer. *Manipulation with Programmable Vector Fields: Design, Fabrication, Control, and Programming of Massively-Parallel Microfabricated Actuator Arrays and Planar Vibratory Parts-Feeders.* PhD thesis, Cornell University, Department of Computer Science, Ithaca, NY 14853, Jan. 1997. Forthcoming.

[4] K.-F. Böhringer, V. Bhatt, and K. Y. Goldberg. Sensorless manipulation using transverse vibrations of a plate. In *Proc. IEEE Int. Conf. on Robotics and Automation (ICRA)*, pages 1989 – 1996, Nagoya, Japan, May 1995. `http://www.cs.cornell.edu/home/karl/VibratoryAlign`.

[5] K.-F. Böhringer, R. G. Brown, B. R. Donald, J. S. Jennings, and D. Rus. Distributed robotic manipulation: Experiments in minimalism. In *Fourth International Symposium on Experimental Robotics (ISER)*, Stanford, California, June 1995. `http://www.cs.cornell.edu/home/brd`.

[6] K.-F. Böhringer, B. R. Donald, and D. Halperin. The area bisectors of a polygon and force equilibria in programmable vector fields, 1996. In preparation.

[7] K.-F. Böhringer, B. R. Donald, and N. C. MacDonald. Single-crystal silicon actuator arrays for micro manipulation tasks. In *Proc. IEEE Workshop on Micro Electro Mechanical Systems (MEMS)*, San Diego, CA, Feb. 1996. `http://www.cs.cornell.edu/home/karl/MicroActuators`.

[8] K.-F. Böhringer, B. R. Donald, R. Mihailovich, and N. C. MacDonald. Sensorless manipulation using massively parallel microfabricated actuator arrays. In *Proc. IEEE Int. Conf. on Robotics and Automation (ICRA)*, pages 826–833, San Diego, CA, May 1994. `http://www.cs.cornell.edu/home/karl/MicroManipulation`.

[9] K.-F. Böhringer, B. R. Donald, R. Mihailovich, and N. C. MacDonald. A theory of manipulation and control for microfabricated actuator arrays. In *Proc. IEEE Workshop on Micro Electro Mechanical Systems (MEMS)*, pages 102–107, Oiso, Japan, Jan. 1994. `http://www.cs.cornell.edu/home/karl/MicroActuators`.

[10] G. Boothroyd, C. Poli, and L. E. Murch. *Automatic Assembly*. Marcel Dekker, Inc., 1982.

[11] A. J. Briggs. An efficient algorithm for one-step planar compliant motion planning with uncertainty. *Algorithmica*, 8(3), 1992.

[12] R. Brooks. A layered intelligent control system for a mobile robot. *IEEE Journal of Robotics and Automation*, RA(2), 1986.

[13] R. C. Brost. Automatic grasp planning in the presence of uncertainty. *Int. Journal of Robotics Research*, 7(1):3–17, 1988.

[14] J. Canny and K. Goldberg. "RISC" for industrial robotics: Recent results and open problems. In *Proc. IEEE Int. Conf. on Robotics and Automation (ICRA)*. IEEE, May 1994.

[15] B. R. Donald. *Error Detection and Recovery in Robotics*, volume 336 of *Lecture Notes in Computer Science*. Springer Verlag, Berlin, 1989.

[16] B. R. Donald. The complexity of planar compliant motion planning with uncertainty. *Algorithmica*, 5(3):353–382, 1990.

[17] B. R. Donald, J. Jennings, and D. Rus. Information invariants for distributed manipulation. In K. Goldberg, D. Halperin, J.-C. Latombe, and R. Wilson, editors, *International Workshop on Algorithmic Foundations of Robotics (WAFR)*, pages 431–459, Wellesley, MA, 1995. K. Peters.

[18] B. R. Donald and P. Xavier. Provably good approximation algorithms for optimal kinodynamic planning for cartesian robots and open chain manipulators. *Algorithmica*, 14(6):480–530, Nov. 1995.

[19] M. A. Erdmann. On a representation of friction in configuration space. *Int. Journal of Robotics Research*, 13(3):240–271, 1994.

[20] M. A. Erdmann. An exploration of nonprehensile two-palm manipulation: Planning and execution. Technical report, Carnegie Mellon University, Pittsburgh, PA, 1996.

[21] M. A. Erdmann and M. T. Mason. An exploration of sensorless manipulation. *IEEE Journal of Robotics and Automation*, 4(4), Aug. 1988.

[22] M. A. Erdmann and M. T. Mason. Nonprehensile manipulation. In *International Workshop on Algorithmic Foundations of Robotics (WAFR)*, Toulouse, France, July 1996.

[23] M. A. Erdmann, M. T. Mason, and G. Vaneček, Jr. Mechanical parts orienting: The case of a polyhedron on a table. *Algorithmica*, 10, 1993.

[24] H. Fujita. Group work of microactuators. In *International Advanced Robot Program Workshop on Micromachine Technologies and Systems*, pages 24–31, Tokyo, Japan, Oct. 1993.

[25] K. Y. Goldberg. Orienting polygonal parts without sensing. *Algorithmica*, 10(2/3/4):201–225, August/September/October 1993.

[26] S. Goyal and A. Ruina. Relation between load and motion for a rigid body sliding on a planar surface with dry friction: Limit surfaces, incipient and asymptotic motion. *Wear*, 1988.

[27] H. Hitakawa. Advanced parts orientation system has wide application. *Assembly Automation*, 8(3), 1988.

[28] R. Hollis and S. E. Salcudean. Lorentz levitation technology: A new approach to fine motion robotics, teleoperation, haptic interfaces, and vibration isolation. In *International Symposium of Robotics Research (ISRR)*, Hidden Valley, PA., Oct. 1993.

[29] L. E. Kavraki. On the number of equilibrium placements of mass distributions in elliptic potential fields. Technical Report STAN-CS-TR-95-1559, Department of Computer Science, Stanford University, Stanford, CA 94305, 1995.

[30] O. Khatib. Real time obstacle avoidance for manipulators and mobile robots. *Int. Journal of Robotics Research*, 5(1):90–99, Spring 1986.

[31] W. Liu and P. Will. Parts manipulation on an intelligent motion surface. In *IROS*, Pittsburgh, PA, 1995.

[32] T. Lozano-Pérez. Spacial planning: A configuration space approach. *IEEE Transactions on Computers*, C-32(2):108–120, Feb. 1983.

[33] T. Lozano-Pérez, M. Mason, and R. Taylor. Automatic synthesis of fine-motion strategies for robots. *Int. Journal of Robotics Research*, 3(1), 1984.

[34] T. McGeer. Passive dynamic walking. *Int. Journal of Robotics Research*, 1990.

[35] R. E. Mihailovich, Z. L. Zhang, K. A. Shaw, and N. C. MacDonald. Single-crystal silicon torsional resonators. In *Proc. IEEE Workshop on Micro Electro Mechanical Systems (MEMS)*, pages 155–160, Fort Lauderdale, FL, Feb. 1993.

[36] P. Moncevicz, M. Jakiela, and K. Ulrich. Orientation and insertion of randomly presented parts using vibratory agitation. In *ASME 3rd Conference on Flexible Assembly Systems*, September 1991.

[37] M. H. Raibert, J. K. Hodgins, R. R. Playter, and R. P. Ringrose. Animation of legged maneuvers: jumps, somersaults, and gait transitions. *Journal of the Robotics Society of Japan*, 11(3):333–341, 1993.

[38] J. Reif and H. Wang. Social potential fields: A distributed behavioral control for autonoomous robots. In K. Goldberg, D. Halperin, J.-C. Latombe, and R. Wilson, editors, *Algorithmic Foundations of Robotics*, pages 431–459. K. Peters, Wellesley, MA, 1995.

[39] E. Rimon and D. Koditschek. Exact robot navigation using artificial potential functions. *IEEE Transactions on Robotics and Automation*, 8(5), October 1992.

[40] K. A. Shaw and N. C. MacDonald. Integrating SCREAM micromechanical devices with integrated circuits. In *Proc. IEEE Workshop on Micro Electro Mechanical Systems (MEMS)*, San Diego, CA, Feb. 1996.

[41] K. A. Shaw, Z. L. Zhang, and N. C. MacDonald. SCREAM I: A single mask, single-crystal silicon process for microelectromechanical structures. In *Transducers — Digest Int. Conf. on Solid-State Sensors and Actuators*, Pacifico, Yokohama, Japan, June 1993.

[42] J. W. Suh, S. F. Glander, R. B. Darling, C. W. Storment, and G. T. A. Kovacs. Combined organic thermal and electrostatic omnidirectional ciliary microactuator array for object positioning and inspection. In *Proc. Solid State Sensor and Actuator Workshop*, Hilton Head, NC, June 1996.

[43] Z. L. Zhang and N. C. MacDonald. An RIE process for submicron, silicon electromechanical structures. *Journal of Micromechanics and Microengineering*, 2(1):31–38, Mar. 1992.

[44] N. B. Zumel and M. A. Erdmann. Nonprehensile two palm manipulation with non-equilibrium transitions between stable states. In *Proc. IEEE Int. Conf. on Robotics and Automation (ICRA)*, Minneapolis, MN, Apr. 1996.